Increasing risks of multiple breadbasket failure under 1.5 and 2°C global warming

Franziska Gaupp*^, Jim Hall*, Dann Mitchell**, Simon Dadson*

** Environmental Change Institute, University of Oxford; ^International Institute for Applied Systems Analysis; ** University of Bristol*

Abstract

The increasingly inter-connected global food system is becoming more vulnerable to production shocks owing to increasing global mean temperatures and more frequent climate extremes. Little is known, however, about the actual risks of multiple breadbasket failure due to extreme weather events. Motivated by the Paris Climate Agreement, this paper quantifies spatial risks to global agriculture in 1.5 and 2°C warmer worlds. This paper focuses on climate risks posed to three major crops - wheat, soybean and maize - in five major global food producing areas. Climate data from the atmosphere-only HadAM3P model as part of the "Half a degree Additional warming, Prognosis and Projected Impacts" (HAPPI) experiment are used to analyse the risks of climatic extreme events. Using the copula methodology, the risks of simultaneous crop failure in multiple breadbaskets are investigated. Projected losses do not scale linearly with global warming increases between 1.5 and 2°C Global Mean Temperature (GMT). In general, whilst the differences in yield at 1.5 versus 2°C are significant they are not as large as the difference between 1.5°C and the historical baseline which corresponds to 0.85°C above pre-industrial GMT. Risks of simultaneous crop failure, however, do increase disproportionately between 1.5 and 2°C, so surpassing the 1.5°C threshold will represent a threat to global food security. For maize, risks of multiple breadbasket failures increase the most, from 6% to 40% at 1.5 to 54% at 2°C warming. In relative terms, the highest simultaneous climate risk increase between the two warming scenarios was found for wheat (40%), followed by maize (35%) and soybean (23%). Looking at the impacts on agricultural production, we show that limiting global warming to 1.5°C would avoid production losses of up to 2 753 million (161 000, 265 000) tonnes maize (wheat, soybean) in the global breadbaskets and would reduce the risk of simultaneous crop failure by 26%, 28% and 19% respectively.

Keywords: Climate Risks, Multiple Breadbasket Failure, Paris Agreement, Copula Methodology

1 Introduction

The Paris Agreement in 2015, in which 197 countries agreed to limit the increase of mean global temperature to 1.5°C rather than 2°C above pre-industrial levels (UNFCCC, 2015), has received considerable interest from the scientific community (i.e., Mitchell et al. 2016b; Rogelj and Knutti 2016; Verschuuren 2016; Schleussner et al. 2016; James et al. 2017). However, so far little research has been done on the impacts of a 1.5°C temperature increase, let alone on the quantification of the differential impacts of 1.5 versus 2°C global warming (James et al., 2017). Quantitative impacts assessments of

the relative benefits of limiting global warming to 1.5ºC are required to support such policies and the scientific community is now encouraged to address research gaps related to a 1.5°C temperature increase, especially to the different impacts at local and regional scales (Rogelj and Knutti, 2016) and the impacts on other industries.

This paper focuses on the climate change impacts on the agricultural sector. Although agriculture is not explicitly mentioned in the Paris Climate Agreement, “safeguarding food security” and the “vulnerabilities of the food production systems to the adverse impacts of climate change” are recognized (UNFCCC, 2015). Agriculture is one of the sectors that will experience the largest negative impacts from climatic change (Porter et al., 2014). Climate trends and specifically climate variability have already negatively impacted agricultural production in many regions (Field and IPCC, 2012; Lobell et al., 2011). On the other hand, it has been estimated that by 2050, an increase of 40% of global food production is necessary to meet the growing demand resulting from population growth and rising calorie intake in developing countries (Verschuuren, 2016). Today, FAO (2014) estimates that 805 million people are undernourished globally, which is one in nine people. In a crisis such as the 2007/08 food price crisis, however, the number of undernourished people increased by 75 million in only four years owing to food price spikes for major crops (Von Braun, 2008). An increasingly interconnected global food system (Puma et al., 2015) and the projected fragility of the global food production system due to climatic change (Fraser et al., 2013) further exacerbate the threats to food security. The potential impact of simultaneous climate extremes on global food security is in particular need of further investigation. Crop losses in a single, main crop producing area, termed a breadbasket, can be offset through trade with other crop-producing regions (Bren d’Amour et al., 2016). If several breadbaskets suffer from negative climate impacts at the same time, however, global production losses might lead to price shocks and trigger export restrictions which amplify the threats to global food security (Puma et al., 2015).

Research has started to focus on the impacts of multiple, interconnected adverse weather events on agricultural production and indirect effects on other industries due to supply chain disruptions and indirect losses such as the financial sector (Lunt et al., 2016; Maynard, 2015). However, more research and information about climate risk distributions and the connection of extreme weather events across the world is needed to estimate the likelihood of multiple breadbasket failures (Bailey and Benton, 2015; Schaffnit-Chatterjee et al., 2010). This paper quantifies simultaneous climate risks to agricultural production in the global breadbaskets under 1.5 and 2°C warming scenarios. Whilst the difference of half a degree might be considered comparatively "small" on an aggregated global level, regional changes can be much larger (Seneviratne et al., 2016). Moreover, changes in extreme events and spatial dependence, which influence global risks such as multiple breadbasket failures, may expose significant differences between the two global mean temperature increments.

This paper uses initial results from the "Half a degree Additional warming, Prognosis and Projected Impacts" (HAPPI) project (Mitchell et al., 2016a). HAPPI provides a set of climate data specifically designed to address the Paris Agreement by simulating scenarios that are 1.5 and 2°C warmer than pre-industrial worlds. It provides a large enough ensemble of climate model runs to enable a thorough assessment of extreme weather and climate-related risks. Results will provide an important contribution to current climate policy discussions about differential impacts at specific global warming levels.

Our paper is organized as follows. In Section 2 we explain the HAPPI experiment and the HadAM3P model which was used in this study. In Section 3 we describe the climate indicators that have been used to assess agricultural risks and how we bias-corrected the data. We introduce the copula methodology used for the multivariate climate risk analysis in this paper and explain how we estimate the impact of climate risks on agricultural production. Section 4 shows the results, which will be further discussed in Section 5. The paper ends in Section 6, which summarizes our findings and gives an outlook to possible future work.

2 Data

2.1 HadAM3P model

Monthly precipitation and maximum temperature data are taken from the global atmosphere only model, HadAM3P (Massey et al., 2015; Pope et al., 2000). HadAM3P was developed by the UK Met Office Hadley Centre and is based on the atmosphere component of HadCM3, a coupled ocean-atmosphere model (Gordon et al., 2000). HadAM3P is run at a global resolution of 1.875° longitude and 1.25° latitude with a 15 minute time step. The model is run via the climate*prediction*.net volunteer distributed computed network (Anderson, 2004) and is, owing to its large ensemble size, well suited to analyse large-scale extreme weather events. Compared to other models from the same modelling family, HadAM3P has improvements in resolution and model physics (Pope and Stratton, 2002). Results of the HadAM3P distributed computing simulations are comparable to results of state of the art global climate model (GCM) simulations (Massey et al., 2015).

2.2 HAPPI experiment

HadAM3P is one of several models used for the HAPPI experiment (Mitchell et al., 2016a) which compares the statistics of extreme weather events simulated for a world which is 1.5 and 2 °C warmer than in pre-industrial (1861-1880) conditions with those of the present day. Driven by several leading atmosphere-only GCMs, HAPPI uses an experimental design similar to CMIP5 and is able to produce large simulation ensembles of high resolution global and regional climate data. Compared to CMIP5 style experiments which use different Representative Concentration Pathways (RCPs) to reach a certain radiative forcing by 2100 and which contain uncertainty in climate model responses, HAPPI uses large sets of simulations under steady forcing conditions to calculate risks at certain warming levels irrespective of the emission pathway. Historical (in this study denoted with HIST) refers to the 2006-2015 decade (which has already experienced a GMT rise of 0.85°C compared to pre-industrial levels (Fischer and Knutti, 2015)), a time period in which ocean temperatures have been

approximately constant but observed Sea Surface Temperatures (SSTs) contain a range of different patterns including El Nino patterns which were used to force the models. Each of the one-decade-simulations in the 50 to 100 member ensembles starts with a different initial weather state which results in 500 to 1000 years of model output. The 1.5°C warming experiment refers to conditions relevant for the 2106-2115 period and uses anthropogenic radiative forcing conditions from RCP2.6 (Van Vuuren et al., 2011) which coincides with a global average temperature response of ~1.5°C relative to pre-industrial levels. Natural radiative forcings are used from the 2006-2015 decade. SSTs in the 1.5°C scenario are calculated by adding the mean projected CMIP5 RCP 2.6 SST changes across 23 models averaged over the 2091-2100 period to observed 2006-2015 SSTs. The 2°C warming scenario refers to 2106-2115 conditions as well and uses a weighted average between the RCP2.5 and RCP4.6 scenarios to reach a ~2°C global mean temperature response, exactly 0.5°C warmer than the 1.5°C scenario. Natural forcings again stay at 2006-2015 levels. For more information on the HAPPI experiment, see (Mitchell et al., 2016a).

Using climate*prediction*.net's large ensemble modelling system, ~150, ~100 and ~120 ensemble members for the historical, 1.5 and 2°C scenario respectively were obtained. Owing to the large number of ensemble members with varied initial conditions, the HAPPI HadAM3P results used in this study are well suited to the analysis of extreme weather events with an improved representation of internal climate variability. Choosing a one-decade time period allows for assessment of the impacts of inter-annual climate variability on agricultural production. Note that the number of ensemble members differs as only ensemble members that were completed on the volunteers' computers could be included. Reasons for non-completion could be hardware failure or termination of the experiment by the volunteer (Massey et al., 2015).

139 *2.3 Historical crop yield and climate data*

140 This study focuses on climate risks to agricultural production in major global breadbaskets.
141 Breadbaskets are important sub-national crop producing regions on a province/state scale in the US,
142 Argentina, China, India and Australia for wheat and the US, Argentina, Brazil, China and India for maize
143 and soybean (see details in Supplementary Information). The regions were chosen based on FAO
144 (2015) country production statistics and official governmental statistics of subnational production. The
145 highest crop producing provinces and states were selected with the premise that the provinces/states
146 of a breadbasket have to be adjacent. For the analysis, the provinces/states were then aggregated to
147 breadbaskets. Europe and Russia/Ukraine were excluded due to a lack of sufficiently long, subnational
148 time-series data. Sub-national, annual crop yield data for all states/provinces of a breadbasket from
149 1967 to 2012 (maize and soybean data in Brazil and India from 1977 and Argentina from 1970) were
150 collected from official governmental databases (Australian Bureau of Statistics, 2015; Conab
151 (Companhia Nacional De Abastecimento) Brazil, 2015; Ministerio de Agricultura, Ganaderia y Pesca de
152 Argentina, 2015; Ministry of Agriculture and Farmers Welfare, Govt. of India, 2015; National Bureau
153 of Statistics of China, n.d.; USDA, 2015). For the analysis, yield data was detrended using a four-
154 parametric logistic function (Gaupp et al., 2016) which has the advantage that it can take on the form
155 of a linear, exponential, damped or logistic trend. Detrended yield data and monthly Princeton re-
156 analysis precipitation and maximum temperature data between 1967 and 2012 (Sheffield et al., 2006)
157 were used to find region- and crop-specific relationships between climate and agricultural production.
158 Princeton re-analysis data is a combination of a number of observation-based datasets and
159 NCEP/NCAR re-analysis data and provides globally consistent, bias-corrected climate data.

160

161

162

3 Methods

3.1 Climate indicator selection

We identified climate indicators which significantly impact three important crops - wheat, maize and soybean - in five breadbaskets around the globe. A climate indicator is a crop and region specific variable based on either monthly maximum temperature or precipitation data which correlates with crop yields.

By concentrating on breadbaskets rather than using the national scale, the region-specific relationship between climate indicator and detrended yield could be determined. This is particularly relevant in large countries where crop production is concentrated in only a few regions. In order to find the most robust climate indicators for each crop and breadbasket, in a first step, an extensive literature review was carried out. Regional case studies were chosen in locations within or very close to the breadbasket areas used in this study. Indicators are mainly average maximum temperature or cumulative precipitation during the crop's growing season (e.g. June to November in India's soybean breadbasket) but also precipitation during the monsoon season (June to September in India's wheat breadbasket) which is stored in the soil and influences wheat growth from October to March (a table with detailed description of climate indicator selection and literature review is in Supplementary Information). In a second step, the choice of the climate indicator was validated through a correlation analysis between the climate re-analysis data and the observed, logistically de-trended (Gaupp et al., 2016) subnational crop yield data on state/province level using the Pearson correlation coefficient, shown in Table 1. The Pearson correlation coefficient is a widely used method to quantify the crop yield-climate relationship (Chen et al., 2014; Luo et al., 2005; Magrin et al., 2005; Podestá et al., 2009; Tao et al., 2008).

Depending on the value and significance of the correlation coefficient, one or two indicators per crop and breadbasket were chosen. In exceptional cases, an indicator was selected when Pearson's *r* showed a non-significant but strong relationship pointing to the same direction as indicated in the

188 literature if it has been described as significant there. Differences can arise through differences
189 between re-analysis data and locally observed climate data, different spatial scales or different
190 statistical methods[1]. Figure 1 shows the indicator selection for each crop and breadbasket as well as
191 the harvesting dates. For the analysis of climate risks, with a climate risk defined as a climate indicator
192 exceeding a critical threshold, climate thresholds were set for each crop, breadbasket and indicator.
193 A simple linear regression between each climate indicator and observed, detrended crop yield was
194 used to define a temperature or precipitation threshold related to the lower 25% detrended yield
195 percentile (see figure SF2 in Supplementary Information). We acknowledge that using a simple linear
196 regression cannot account for the possibility of non-linear relationships between climate indicator and
197 crop yield or the interaction between precipitation and temperature. Applying a simple linear
198 regression allows one to identify the most relevant climate indicators for different crop yields (Tao,
199 2008) which serves the purpose of this paper. Similar to other papers in the field (e.g. Lobell et al.,
200 2011) this study does not aim to predict actual future yields but to estimate the future impact of
201 climate on agricultural production. In contrast to process-based models (e.g. Asseng et al., 2015;
202 Rosenzweig et al., 2014; Schleussner et al., 2016a), which represent key dynamic processes affecting
203 crop yields, our approach is based on empirical relationships between location- and crop-specific
204 climate indicators and crop yields. As Lobell and Asseng (2017) have shown, there are no systematic
205 difference between the predicted sensitivities to warming between the two approaches up to 2°C
206 warming. Empirical models are able to assess the climate-yield relationship location-specifically.
207 Process-based models are typically better in understanding the interaction between crop genetics,
208 management options and climate but might ignore factors that are important to crop growth in some
209 seasons or specific environments.

[1] This is why in reports such as the IPCC reports (Allen et al., 2019; IPCC, 2014), different models are used and compared to give policy recommendations and model inter-comparison projects such as ISIMIP (www.isimip.org) or AgMIP (www.agmip.org) have been conducted. Lobell and Asseng (2017) compared process based and statistical crop models and found no systematic difference between predicted sensitivities to warming between the two model types up to a 2 degree warming.

To account for uncertainties in the sample statistics of the HAPPI data, the data were bootstrapped 1000 times for the threshold exceedance calculation. Results in Figure 2 show the simulation mean. A breadbasket is experiencing a climate risks for a crop as soon as one of the temperature or precipitation based indicators is exceeding the threshold. The breadbasket-specific relationship between temperature and precipitation is accounted for through the copula correlation structure explained in Section 3.3.

3.2 Bias-correction

In order to quantify the likelihood of threshold exceedance of different climate indicators, the HadAM3P model output has to be comparable to the observed historical climate used for setting these thresholds. Therefore, both historical and future experiment results were calibrated using a simple bias-correction method (Hawkins et al., 2013; Ho, 2010) which corrects mean and variability biases of the climate indicators distributions using the Princeton re-analysis data (Sheffield et al., 2006) as calibration dataset:

$$I_{BC}(t) = \overline{O_{REF}} + \frac{\sigma_{O,REF}}{\sigma_{I,REF}} \left(I_{REF}(t) - \overline{I_{REF}}\right) \quad (1)$$

$$I_{FUT,BC}(t) = \overline{O_{REF}} + \frac{\sigma_{O,REF}}{\sigma_{I,REF}} \left(I_{FUT}(t) - \overline{I_{REF}}\right) \quad (2)$$

I_{BC} denotes the HAPPI HadAM3P bias-corrected climate indicator, O_{REF} and I_{REF} the observational Princeton dataset and HAPPI HadAM3P historical raw climate indicators and I_{FUT} represents the 1.5 or 2°C raw climate indicator. This method has the advantage of being simple to calculate and being independent of the shape of the climate variable distribution (Hawkins et al., 2013). It is used widely in agricultural modelling (Navarro-Racines et al., 2016). Although for precipitation usually a more

231 complicated calibration method has to be applied as it cannot take negative values, in this case it was
232 possible as we use aggregated precipitation values which never reach zero. HadAM3P generally
233 overestimated temperature compared to the Princeton dataset with HadAM3P maximum
234 temperature being between 7 and 57% higher than Princeton in all breadbaskets. Precipitation is
235 underestimated in the maize and soybean breadbaskets by between 2 and 30%. Precipitation for
236 wheat, which has a different growing season, is both higher and lower than the reference dataset
237 (between 40% lower in Australia and 37% higher in the US breadbasket).

238

239 *3.3 Regular vine copulas*

240 In this study, climate indicators based on historical Princeton re-analysis data were used to estimate
241 the spatial dependence structure between the five breadbaskets to avoid biases in inter-regional
242 correlation in the HadAM3P climate model. As the dependence structure of the HAdAM3P climate
243 indicators in the different breadbaskets did not change between historical and warming scenarios, we
244 kept the historical dependence structure constant in the 1.5 and 2°C scenarios. Changes in
245 simultaneous climate risks between scenarios occur due to changes in mean and variance of the
246 underlying marginal distributions of the climate indicators based on HadAM3P data.
247 In order to estimate risks of multiple breadbasket failure owing to joint climate extremes in major crop
248 production areas[2], the spatial dependence structure of the global breadbasket's climate indicators
249 was modelled using regular vine (RVine) copulas (Aas et al., 2009; Dißmann et al., 2013; Kurowicka
250 and Cooke, 2006). RVines are a flexible class of multivariate copulas which are able to model complex
251 dependencies in larger dimensions. They are based on Sklar's theorem (Sklar, 1959) which states that
252 any multivariate distribution *F* can be written as

[2] We acknowledge that heterogeneity is lost with aggregation to breadbaskets. However, we made sure that the relationship between climate indicators and yields were robust between our states/provinces, the aggregated breadbasket scale and local studies taken from the literature.

253

$$\boldsymbol{F}(\boldsymbol{x_1}, \dots, \boldsymbol{x_n}) = \boldsymbol{C}[\boldsymbol{F_1}(\boldsymbol{x_1}), \dots, \boldsymbol{F_n}(\boldsymbol{x_n})] \quad (3)$$

254 with marginal probability distributions $F_1(x_1)$, …, $F_n(x_n)$ and C denoting an n-dimensional copula, a
255 multivariate distribution on the unit hypercube $[0,1]^2$ with uniform marginal distributions. Vine
256 copulas are constructed using conditional and unconditional bivariate pair-copulas from a set of
257 copula families with distinct dependence structures (Aas et al., 2009; Joe, 1997). A set of linked RVine
258 trees describes the factorisation of the copula's multivariate density function (Bedford and Cooke,
259 2002). An n-dimensional RVine model consists of (n-1) trees including N_i nodes and E_{i-1} edges which
260 join the nodes. The tree structure is built according to the proximity condition which means that if an
261 edge connects two nodes in tree j+1, the corresponding edges in tree j share a node (Bedford and
262 Cooke, 2002). The first tree consist of n-1 pairs of variables with directly modelled distributions. The
263 second tree identifies n-2 variable pairs with a distribution modelled by a pair-copula conditional on a
264 single variable which is determined in the second tree. Proceeding in this way, the last tree consist of
265 a single pair of variables with a distribution conditional on all remaining variables, defined by a last
266 pair-copula (Dißmann et al., 2013). The RVine tree structure, the pair-copula families and the copula
267 parameters are estimated in an automated way starting with the first tree. The tree is selected using
268 a maximum spanning tree algorithm and Kendall's tau as edge weights. The best fitting pair-copula
269 family is chosen using the Akaike Information Criterion (Akaike, 1973) and copula parameters are
270 estimated using Maximum Likelihood Estimation (MLE). In this study we chose from six different
271 copula families representing different types of tail dependencies to capture the exact patterns of
272 dependence between the different climate indicators in the crop breadbaskets: Gaussian, Clayton,
273 Student-t, Gumbel, Joe and Frank copulas (Nelsen, 2007).
274

275 *3.4 Impact on agricultural production*

We analyse events where the climatic conditions in all five breadbaskets are associated with losses in agricultural yields. We identify a 'breadbasket failure' event as being when the climatic conditions are at least as severe as those conditions associated with the 25 percentile of the logistically detrended yields (with detrended yields as residuals of the non-linear logistic regression with a residual mean equal to zero). The crop production loss for an event of this severity is the 25 percentile of the logistically detrended yield multiplied with the 2012 harvested area. Given that we identify climatic events that are *at least* as severe as this condition, our estimated loss is the lower bound on the loss, i.e. the minimum expected loss. Minimum expected losses are then defined as the sum of crop losses in all five breadbaskets multiplied with the joint probability that climate thresholds are exceeded in all regions simultaneous as shown in Equation 4:

$$\boldsymbol{Minimum\ expected\ losses} \geq \sum_{\boldsymbol{i}}^{\boldsymbol{BB}} \left(|\, \boldsymbol{y25_i}| \cdot \boldsymbol{area_{i,2012}} \right) \cdot \boldsymbol{p_5} \tag{4}$$

with

$$p_5 = P\left(Clim_1 \gtrless t_{Clim_1},\ Clim_2 \gtrless t_{Clim_2},\quad Clim_3 \gtrless t_{Clim_3}, Clim_4 \gtrless t_{Clim_4}, Clim_5 \gtrless t_{Clim_5} \right)$$
$$= C\left[F_1\left(t_{clim_1}\right), F_2\left(t_{clim_2}\right), F_3\left(t_{clim_3}\right), F_4\left(t_{clim_4}\right), F_5\left(t_{clim_5}\right) \right]$$

with $y25_i$ as the 25 percentile of logistically detrended yields in the breadbasket *i* which was used to define climate thresholds and which indicates a minimum yield loss, $area_{i,2012}$ as the 2012 harvested area in breadbasket *i* and with p_5 as the probability of all five breadbaskets exceeding the climate thresholds in the same year. $Clim_i$ denotes the temperature or precipitation-based climate indicator, associated with the 25 percentile of the detrended yields. In case that a breadbasket has two indicators for a crop, the exceedance of at least one of the climate thresholds t_{clim_i} is counted as threshold exceedance in the breadbasket. *C* denotes the copula.

299

300 # 4 Results

301

302 ## *4.1 Changes in climate risks to agriculture under 1.5 and 2°C global warming*

303 The change of climate risks to major crops in the global breadbaskets were examined for each region
304 and crop separately comparing historical risks with risks associated with a 1.5 and 2°C global warming,
305 shown in Figure 2. As expected from an increase of global mean temperature, temperature based
306 climate risks are increasing, but to different extents depending on the region. Precipitation signals
307 associated with 1.5 and 2°C warming are less clear. While precipitation based climate risks in the US
308 and Brazil increase in both scenarios for the summer crops maize and soybean, precipitation in
309 Argentina does not significantly change. Risks in China and India decrease due to an increase in
310 monsoon precipitation. For wheat, precipitation-based climate risks only increase in Australia.

311 The decrease of precipitation-based climate risks to wheat in the US and China, and the increase in
312 the Australian breadbaskets for both warming scenarios mostly coincide with findings of a previous
313 study (Gaupp et al., in review) which examined climate risk trends in the past. In India and China,
314 wheat is indirectly impacted by the summer monsoon rainfall which provides stored soil moisture for
315 the "rabi" wheat crop. Although precipitation between June and September in the Chinese
316 breadbasket showed a decrease in the recent past, in a 1.5 and 2°C warmer world precipitation during
317 monsoon months in the Chinese breadbasket is projected to increase. This coincides with (Lv et al.,
318 2013) who project a decrease in precipitation in China during the wheat growing season between the
319 2000s and 2030s and a consistent precipitation increase from the 2030s to the 2070s. In India, rainfall
320 during summer monsoon months (June to September) showed a decreasing decadal trend in the
321 recent past (Guhathakurta et al., 2015) which was reflected in an increasing climate risk for wheat in
322 India in the past (Gaupp et al., in review). In the future, however, monsoon precipitation is projected
323 to increase under all RCP scenarios in CMIP5 projections (Jayasankar et al., 2015; Menon et al., 2013)

which coincides with decreasing precipitation climate risks to wheat in the Indian breadbasket found in this study. However, precipitation-based risks in India and China might be underestimated in this study because of the HAPPI experiment structure which has fixed SSTs driving the model, rather than a fully couple ocean simulation. This often leads to variability in land-ocean driven cycles not changing much and thereby to an underestimation of precipitation variability during the monsoon months. CMIP5 models project both increasing and decreasing standard deviations of monsoon precipitation in India for RCP 2.6 and 4.5. In Australia, precipitation in the wheat growing season is projected to decrease following different CMIP5 models under RCP4.5 (Ummenhofer et al., 2015) which our study confirms through increased precipitation-based climate risks. Temperature risks are increasing in all temperature sensitive breadbaskets with stronger increases in India and Australia than in Argentina. Our estimates of climate risks to wheat production coincide with results of crop model experiments in other studies. Asseng et al. (2015) compared results of 30 wheat crop simulation models in 30 main wheat producing locations without water stress, focussing only on the effect of temperature. All models showed yield losses at a 2°C warming, which coincides with our temperature-based climate risk increases in India, Australia and Argentina. Rosenzweig et al. (2018) and Ruane et al. (2018) used HAPPI climate data and other climate model experiments from CMIP5 to compare climate impacts on crops under a 1.5°C and 2°C warming using process-based crop models. They found wheat yield losses smaller than 5% in the North American Great Plains, but larger losses in Australia and Argentina under 1.5°C warming. In India and China the models showed yield increases in a 1.5°C world. Challinor et al. (2014) came to similar conclusions in a meta-analysis of crop yield under climate change. He found no changes in wheat yields under a 1.5°C warming in tropical regions but a slight decrease under 2°C. In temperate regions, such as the US, China or Argentina, wheat yields are projected to decrease for both warming levels, when adaptation strategies such as irrigation, planting times of crop varieties are not considered.

For soybean, precipitation-based climate risks in South America increase in Brazil but do not change notably in Argentina. This coincides with findings from other CMIP5 studies (Barros et al., 2015; IPCC, 2014). In the US, CMIP5 models show a small, not significant increase in annual precipitation (IPCC, 2014)) which can be seen in HadAM3P as well. Precipitation during the soybean growing season, on the other hand, is projected to decrease in both 1.5 and 2°C scenarios which results in higher climate risks. In China and India, soybean growing seasons are directly aligned with the summer monsoon. Hence, precipitation-based soybean climate risks decrease due to the above discussed increase in monsoon precipitation. Temperature based risks, on the other hand, increase significantly in the US, Argentina and India. Those temperature and precipitation changes translated into yield changes in several crop model experiments for rainfed and irrigated soybean. The models show slight yield decreases over the interior of Northern America but small increases towards the eastern US in a 1.5°C scenario for rainfed soybean. In Brazil and Argentina, soybean shows both increases and decreases under a 1.5°C warming and in the Indian breadbasket, soybean yields are projected to increase. In China, yields are projected to increase in the North, but decrease in the South. Models for irrigated crop that also include CO_2 benefits, yields are projected to increase (Ruane et al., 2018). Under a 2°C warming, GCMs revealed yield increases when CO_2 effects were considered as they largely overcome increased temperature risks (Ruane et al., 2018; Schleussner et al., 2016a).

For maize, climate risks show very similar patterns to soybean as the two summer crops have similar growing seasons and indicators. Additional to the soybean climate indicators, maize in the Chinese breadbasket is sensitive to temperature. Owing to those local precipitation changes and temperature rise, global crop models (GCMs) have shown declines in maize yields in all five breadbaskets in both a 1.5 and 2°C warmer world (Ruane et al., 2018; Schleussner et al., 2016a). In contrast to soybean, maize is not able to capture the same level of CO_2 benefits and hence yields decrease further under in a 2°C world. Those finding coincide with results of the meta-study by Challinor et al. (2014).

One of the major concerns in studies of the difference between a 1.5 and 2°C global warming is the significance of the difference between the temperature increments (James et al., 2017). The difference between climate risks for 1.5 and 2°C in this study was tested with the student two-sample Kolmogorov-Smirnov (KS) test which tests the null hypothesis that both distributions of resampled threshold exceedance are drawn from the same distribution. Results showed significant differences for all indicators and crops at the 0.001 significance level between the two warming levels. The KS test allows for robust statements about the difference between climate risks under 1.5 and 2°C warming even if there is an overlap of uncertainty bands (Schleussner et al., 2016a). Error bars are small compared to the absolute change in climate threshold exceedance with the exception of precipitation risks in Argentina for soybean and maize. Figure 2 also compares the difference in changes from historical climate for both global mean temperature increases. Across all three crops, we found stronger signals for temperature based risks than for precipitation based risks which show smaller, both positive and negative signals. Additionally, the difference between the 1.5 and 2°C warming is more pronounced in temperature based indicators with the largest difference in the Indian soybean breadbasket (26% points). The difference in precipitation risk changes between the two warming scenarios lies between 0 and 6% points. What stands out is the difference between 1.5 and 2°C for precipitation risks in Brazil. In contrast to other climate indicators, precipitation between December and February and March in Brazil shows a significantly stronger difference from historical data to 1.5°C than to 2°C.

4.2 Increasing risks of multiple breadbasket failure

Having analysed individual changes of climate risks in the global wheat, soybean and maize breadbaskets for 1.5 and 2°C enables us to calculate joint climate risks on a global scale. Figure 3 shows the largest increase in risks of simultaneous crop failure (resulting from climate exceeding a crop- and region-specific threshold) in the global breadbaskets for maize, followed by soybean and wheat. For all three crops the likelihoods that none or just one of the breadbaskets experiences climate risks

399 decreases to (nearly) zero. For wheat and soybean, the likelihoods of breadbaskets experiencing
400 detrimental climate change increases significantly from the historical scenario to 1.5°C and even more
401 assuming 2°C warming. The figure can be interpreted as a discrete probability distribution with the
402 sum of all breadbasket threshold exceedances adding up to 1. The shape of the distribution stays
403 roughly the same across warming scenarios with higher probabilities that parts of the breadbaskets
404 exceed the thresholds and smaller likelihoods in the extremes. While the historical baseline climate
405 still shows the probability for zero simultaneous climate risks, for higher temperature scenarios these
406 likelihoods disappear. The average threshold exceedance increases significantly (measured using the
407 KS-test), more for soybean than for wheat. For maize, likelihoods of simultaneous climate risks
408 increase strongly. Under the 2°C scenario the likelihood of all five breadbaskets suffering detrimental
409 climate is the highest. For wheat, which shows the smallest simultaneous climate risks, the return
410 period for all five breadbaskets exceeding their climate thresholds decreases from 43 years (or 0.023
411 annual probability under historical conditions to 21 years (0.047) in a 1.5°C scenario and further down
412 to around 15 years (0.066) under 2°C. Soybean has a return period of simultaneous climate risks in all
413 breadbaskets of around 20 years (0.049 today which decreases to 9 (0.116) and 7 years (0.143 in a 1.5
414 and 2°C warmer world respectively. Maize risks are highest in our study with an initial return period
415 of 16 years (0.061), decreasing to less than 3 (0.39) and less than 2 years (0.538) under future global
416 warming. In general, one can say that whilst the differences in yield at 1.5 vs 2°C are significant they
417 are not as large as the difference between 1.5 and historical. Risk of simultaneous crop failure,
418 however, do increase disproportionately between 1.5 and 2 degrees and this is important because
419 correlated risks lead to disproportionately high impacts.

420 To illustrate the effects of simultaneous climate risks in a 1.5 and a 2°C warmer world, we estimated
421 the impacts on agricultural production. Simultaneous crop failure in all breadbaskets, defined as the
422 25 percentile of detrended yield, would add up to at least 9.86 million tons of soybean losses, 19.75
423 million tons of maize losses and 8.59 million tons of wheat losses assuming 2012 agricultural area.
424 Historical examples of global crop production shocks include 7.2 million tons soybean losses in

425 1988/99 and 55.9 million tons maize losses in 1988 which were mostly caused by low rainfall and high
426 temperatures during summer growing season in the US (Bailey and Benton, 2015). Historical global
427 wheat production shocks include 36.6 million tons wheat losses in 2003 mostly caused by heat waves
428 and drought in spring in Europe and Russia but also by reduced acreage due to drought or winterkill
429 in Europe, India and China (Bailey and Benton, 2015). Maize and wheat losses in this study are lower
430 than in historical cases as our breadbaskets only account for 38% and 52% of global production
431 respectively. Soybean in this study accounts for 80% of global production. Combining absolute losses
432 with likelihoods of simultaneous climate risks, we calculated expected crop losses following Equation
433 4. For all three crops, expected crop losses are significantly higher under the 2°C than under the 1.5°C
434 scenario. Under a scenario of 2°C mean global warming, expected wheat, maize and soybean losses
435 are projected to be 161 000, 2 753 000 and 265 000 tonnes higher than if global temperature
436 increases are limited to 1.5°C. This equals total annual maize production in Uganda, the world's 33rd
437 largest maize producer in 2012. The difference of wheat losses is larger than Bolivia's annual total
438 production in 2012 (145 000 tonnes) and the increase of expected soybean losses is comparable to
439 Mexico's annual production (248 000 tonnes), the world's 20th biggest soybean producer (FAO, 2015).

440 To test for the influence of inter-dependence between the climate indicators in the different
441 breadbaskets on the results of this analysis, we excluded the correlations between them. We assumed
442 independence between the breadbaskets, but still accounted for the negative correlation between
443 temperature and precipitation indices within one breadbasket. Supplementary Figure SF3 illustrates
444 the difference between independence and correlation. Between the three crops, no consistent
445 pattern was found between dependent and independent cases. The only crop that shows significant
446 differences is soybean with smaller likelihoods in the extremes when dependence is excluded. This
447 means that the likelihood of all five soybean breadbaskets experiencing detrimental climate in one
448 year is underestimated if correlations between the breadbaskets are not considered in a risk analysis.
449 Expressed in expected production losses, the losses are up lo 190 000 tonnes higher in the dependent

450 case which is more than what the 22nd largest soybean producer harvests annually (FAO, 2015). For
451 wheat and maize, the difference between the dependencies was mostly not significant.

452

453 5 Discussion

454 Our results illustrate future climate conditions under two warming scenarios in the global
455 breadbaskets and investigate simultaneous climate risks affecting three major crops. The study
456 focused explicitly on the climate impact on crop yields. The effects of other factors such as soil quality,
457 land management, land use or technology were held constant under future warming scenarios.
458 Therefore, our estimates of crop production losses have to be interpreted with care. By not explicitly
459 including CO_2 concentrations, for instance, the CO_2 fertilizer effect which increases productivity in
460 wheat and soybean and to a certain extent in maize (Schleussner et al., 2016a) was not taken into
461 account. The effects of climatic change on plant phenology were not considered. In China, for instance,
462 the flowering date of wheat is projected to advance owing to increased temperatures and the gain-
463 filling period will shorten which might further reduce yields (Lv et al., 2013). By holding harvested area
464 constant at 2012 levels, shifts in land use and cropped area in response to projected climatic changes
465 (Nelson et al., 2014; Schmitz et al., 2014) were not considered. Owing to a lack of subnational historic
466 time series of irrigated crop yields, irrigation was not specifically taken into account in setting climate
467 risk thresholds. This was acceptable in this study as, even without considering irrigation, the
468 correlation coefficients between observed, detrended yields and climate indicators were mostly
469 significant. A large share of the regions in this study are completely rain-fed. In other regions such as
470 India or the US, irrigated crops still show correlations with rainfall (Pathak and Wassmann, 2009) or
471 no significant difference to rain-fed crops at all (Zhang et al., 2015). Results of the analysis of
472 simultaneous climate risks may vary depending on the climate indicator selection. The two-step
473 approach of pre-selecting potential indicators in a literature review and verification through the
474 correlation analysis with re-analysis climate data and observed historical yield data represents a

robust way of indicator selection. However, including different climate variables such as number of days above a crop dependent heat threshold (Schlenker and Roberts, 2009; Tack et al., 2015; Zhang et al., 2015) or dry spell length (Hernandez et al., 2015; Ramteke et al., 2015; Schleussner et al., 2016a) might lead to different results. So far, the HAPPI project only provides monthly data which limited the climate variable choice. In order to reduce uncertainties, we bootstrapped the climate indicators and repeatedly simulated the copula models. However, results from 1.5 and 2°C warming scenarios vary between different GCMs (Schleussner et al., 2016a). A comparison with additional climate models from the HAPPI project will further improve the robustness of the results.

6 Conclusion

This study found disproportionally increasing future risks of simultaneous crop failure in the global wheat, maize and soybean breadbaskets in a 1.5 and 2°C warmer world using results of the HadAM3P atmospheric model as part of the HAPPI experiment. Increases in temperature-based climate risks were found to be stronger than precipitation-based risks which showed different signals depending on crop and region. Using the copula methodology, it was possible to capture dependence structures between regions and to calculate joint climate risks in the major crop producing areas. Additionally, the copula analysis accounted for the region-specific relationships between temperature and precipitation. Strongest increases in simultaneous climate risks were found for maize where return periods of simultaneous crop failure decrease from 16 years in the past to less than 3 and less than 2 years under 1.5 and 2°C warming. In percentage terms, the largest increase of simultaneous climate threshold exceedance in all five breadbaskets between the two warming scenarios was found for wheat (40%), followed by maize (35%) and soybean (23%). Looking at the impacts on crop production, the study showed that limiting global warming to 1.5°C would avoid production losses of up to 2 753 million (161 000, 265 000) tonnes maize (wheat, soybean) in the main production regions.

Our study represents an important first step in the analysis of differential temperature increases of 1.5 and 2°C and their impacts on agricultural production. Compared to climate studies which often focus on average annual values, this study focused on crop growth periods which may show opposite signals to annual means – as shown here for soybean in the US - and therefore added valuable information to existing studies.

Results are based on HadAM3P, the first model in the HAPPI experiment set up. Including outputs from additional climate models will give more robust information on future climate risks. Additionally, further analysis of the ability of climate models to accurately model spatial dependence between regions is needed. This study used historical dependence to avoid biases in spatial correlation and kept dependence constant under future scenarios. Some literature, however, suggests that teleconnection patterns might change, i.e. owing to changes in El Niño Southern Oscillation (ENSO) (Cai et al., 2014; Power et al., 2013), which could then alter the spatial climate dependence structure in the breadbaskets. Future work (under preparation) will look into climate risks under different ENSO phases.

This paper provides insights into risks of multiple breadbasket failure under 1.5 and 2°C warming which can contribute to current climate policy discussions and potentially provides useful information for the Intergovernmental Panel on Climate Change (IPCC) Special Report on the impact of 1.5°C global warming commissioned by the UN-FCCC after the Paris Agreement.

References

Aas, K., Czado, C., Frigessi, A., Bakken, H., 2009. Pair-copula constructions of multiple dependence. Insur. Math. Econ. 44, 182–198. https://doi.org/10.1016/j.insmatheco.2007.02.001

Akaike, H., 1973. Information theory and an extension of the maximum likelihood principle. Á In: Petran, BN and Csáki, F, in: International Symposium on Information Theory, Second Edition. Akadémiai Kiadi, Budapest, Hungary, Pp. 267Á281.

Allen, M., Antwi-Agyei, P., Aragon-Durand, F., Babiker, M., Bertoldi, P., Bind, M., Brown, S., Buckeridge, M., Camilloni, I., Cartwright, A., 2019. Technical Summary: Global warming of 1.5° C. An IPCC Special Report on the impacts of global warming of 1.5° C above pre-industrial levels and related global greenhouse gas emission pathways, in the context of

strengthening the global response to the threat of climate change, sustainable development, and efforts to eradicate poverty.
Anderson, D.P., 2004. Boinc: A system for public-resource computing and storage, in: Grid Computing, 2004. Proceedings. Fifth IEEE/ACM International Workshop On. IEEE, pp. 4–10.
Asseng, S., Ewert, F., Martre, P., Rötter, R.P., Lobell, D.B., Cammarano, D., Kimball, B.A., Ottman, M.J., Wall, G.W., White, J.W., Reynolds, M.P., Alderman, P.D., Prasad, P.V.V., Aggarwal, P.K., Anothai, J., Basso, B., Biernath, C., Challinor, A.J., De Sanctis, G., Doltra, J., Fereres, E., Garcia-Vila, M., Gayler, S., Hoogenboom, G., Hunt, L.A., Izaurralde, R.C., Jabloun, M., Jones, C.D., Kersebaum, K.C., Koehler, A.-K., Müller, C., Naresh Kumar, S., Nendel, C., O'Leary, G., Olesen, J.E., Palosuo, T., Priesack, E., Eyshi Rezaei, E., Ruane, A.C., Semenov, M.A., Shcherbak, I., Stöckle, C., Stratonovitch, P., Streck, T., Supit, I., Tao, F., Thorburn, P.J., Waha, K., Wang, E., Wallach, D., Wolf, J., Zhao, Z., Zhu, Y., 2015. Rising temperatures reduce global wheat production. Nat. Clim. Change 5, 143–147. https://doi.org/10.1038/nclimate2470
Australian Bureau of Statistics, 2015. Historical Selected Agriculture Commodities. URL http://www.abs.gov.au/
Bailey, R., Benton, T., 2015. Extreme weather and resilience of the global food system. Final Project Report from the UK-US Taskforce on Extreme Weather and Global Food System Resilience, The Global Food Security programme, UK.
Barros, V.R., Boninsegna, J.A., Camilloni, I.A., Chidiak, M., Magrín, G.O., Rusticucci, M., 2015. Climate change in Argentina: trends, projections, impacts and adaptation: Climate change in Argentina. Wiley Interdiscip. Rev. Clim. Change 6, 151–169. https://doi.org/10.1002/wcc.316
Bedford, T., Cooke, R.M., 2002. Vines: A new graphical model for dependent random variables. Ann. Stat. 1031–1068.
Bren d'Amour, C., Wenz, L., Kalkuhl, M., Christoph Steckel, J., Creutzig, F., 2016. Teleconnected food supply shocks. Environ. Res. Lett. 11, 035007. https://doi.org/10.1088/1748-9326/11/3/035007
Cai, W., Borlace, S., Lengaigne, M., Van Rensch, P., Collins, M., Vecchi, G., Timmermann, A., Santoso, A., McPhaden, M.J., Wu, L., others, 2014. Increasing frequency of extreme El Niño events due to greenhouse warming. Nat. Clim. Change 4, 111–116.
Challinor, A.J., Watson, J., Lobell, D.B., Howden, S.M., Smith, D.R., Chhetri, N., 2014. A meta-analysis of crop yield under climate change and adaptation. Nat. Clim. Change 4, 287.
Chen, H., Wang, J., Huang, J., 2014. Policy support, social capital, and farmers' adaptation to drought in China. Glob. Environ. Change 24, 193–202. https://doi.org/10.1016/j.gloenvcha.2013.11.010
Conab (Companhia Nacional De Abastecimento) Brazil, 2015. Séries históricas. URL http://www.conab.gov.br
Dißmann, J., Brechmann, E.C., Czado, C., Kurowicka, D., 2013. Selecting and estimating regular vine copulae and application to financial returns. Comput. Stat. Data Anal. 59, 52–69. https://doi.org/10.1016/j.csda.2012.08.010
FAO, 2015. Statistical database.
FAO (Ed.), 2014. Strengthening the enabling environment for food security and nutrition, The state of food insecurity in the world. FAO, Rome.
Field, C.B., IPCC (Eds.), 2012. Managing the risks of extreme events and disasters to advance climate change adaption: special report of the Intergovernmental Panel on Climate Change. Cambridge University Press, New York, NY.
Fischer, E.M., Knutti, R., 2015. Anthropogenic contribution to global occurrence of heavy-precipitation and high-temperature extremes. Nat. Clim. Change 5, 560–564. https://doi.org/10.1038/nclimate2617
Fraser, E.D.G., Simelton, E., Termansen, M., Gosling, S.N., South, A., 2013. "Vulnerability hotspots": Integrating socio-economic and hydrological models to identify where cereal production

578 may decline in the future due to climate change induced drought. Agric. For. Meteorol. 170,
579 195–205. https://doi.org/10.1016/j.agrformet.2012.04.008
580 Gaupp, F., Pflug, G., Hochrainer-Stigler, S., Hall, J., Dadson, S., 2016. Dependency of Crop Production
581 between Global Breadbaskets: A Copula Approach for the Assessment of Global and
582 Regional Risk Pools. Risk Anal.
583 Gordon, C., Cooper, C., Senior, C.A., Banks, H., Gregory, J.M., Johns, T.C., Mitchell, J.F., Wood, R.A.,
584 2000. The simulation of SST, sea ice extents and ocean heat transports in a version of the
585 Hadley Centre coupled model without flux adjustments. Clim. Dyn. 16, 147–168.
586 Guhathakurta, P., Rajeevan, M., Sikka, D.R., Tyagi, A., 2015. Observed changes in southwest
587 monsoon rainfall over India during 1901-2011: TREND IN SOUTHWEST MONSOON RAINFALL
588 OVER INDIA. Int. J. Climatol. 35, 1881–1898. https://doi.org/10.1002/joc.4095
589 Hawkins, E., Osborne, T.M., Ho, C.K., Challinor, A.J., 2013. Calibration and bias correction of climate
590 projections for crop modelling: An idealised case study over Europe. Agric. For. Meteorol.
591 170, 19–31. https://doi.org/10.1016/j.agrformet.2012.04.007
592 Hernandez, V., Moron, V., Riglos, F.F., Muzi, E., 2015. Confronting farmers' perceptions of climatic
593 vulnerability with observed relationships between yields and climate variability in Central
594 Argentina. Weather Clim. Soc. 7, 39–59.
595 Ho, C.K., 2010. Projecting extreme heat-related mortality in Europe under climate change.
596 IPCC, 2014. Climate Change 2014–Impacts, Adaptation and Vulnerability: Regional Aspects.
597 Contribution of Working Group II to the Fifth Assessment Report of the Intergovernmental
598 Panel on Climate Change. Cambridge University Press, Cambridge, United Kingdom and New
599 York, NY, USA.
600 James, R., Washington, R., Schleussner, C.-F., Rogelj, J., Conway, D., 2017. Characterizing half-a-
601 degree difference: a review of methods for identifying regional climate responses to global
602 warming targets: Characterizing half-a-degree difference. Wiley Interdiscip. Rev. Clim.
603 Change e457. https://doi.org/10.1002/wcc.457
604 Jayasankar, C.B., Surendran, S., Rajendran, K., 2015. Robust signals of future projections of Indian
605 summer monsoon rainfall by IPCC AR5 climate models: Role of seasonal cycle and
606 interannual variability: FUTURE PROJECTIONS OF ISMR. Geophys. Res. Lett. 42, 3513–3520.
607 https://doi.org/10.1002/2015GL063659
608 Joe, H., 1997. Multivariate models and multivariate dependence concepts. CRC Press.
609 Kurowicka, D., Cooke, R.M., 2006. Uncertainty analysis with high dimensional dependence
610 modelling. John Wiley & Sons.
611 Lobell, D.B., Asseng, S., 2017. Comparing estimates of climate change impacts from process-based
612 and statistical crop models. Environ. Res. Lett. 12, 015001.
613 Lobell, D.B., Schlenker, W., Costa-Roberts, J., 2011. Climate trends and global crop production since
614 1980. Science 333, 616–620.
615 Lunt, T., Jones, A.W., Mulhern, W.S., Lezaks, D.P.M., Jahn, M.M., 2016. Vulnerabilities to agricultural
616 production shocks: An extreme, plausible scenario for assessment of risk for the insurance
617 sector. Clim. Risk Manag. 13, 1–9. https://doi.org/10.1016/j.crm.2016.05.001
618 Luo, Q., Bellotti, W., Williams, M., Bryan, B., 2005. Potential impact of climate change on wheat yield
619 in South Australia. Agric. For. Meteorol. 132, 273–285.
620 https://doi.org/10.1016/j.agrformet.2005.08.003
621 Lv, Z., Liu, X., Cao, W., Zhu, Y., 2013. Climate change impacts on regional winter wheat production in
622 main wheat production regions of China. Agric. For. Meteorol. 171, 234–248.
623 Magrin, G.O., Travasso, M.I., Rodríguez, G.R., 2005. Changes in climate and crop production during
624 the 20th century in Argentina. Clim. Change 72, 229–249.
625 Massey, N., Jones, R., Otto, F.E.L., Aina, T., Wilson, S., Murphy, J.M., Hassell, D., Yamazaki, Y.H., Allen,
626 M.R., 2015. weather@home-development and validation of a very large ensemble modelling
627 system for probabilistic event attribution: weather@home. Q. J. R. Meteorol. Soc. 141,
628 1528–1545. https://doi.org/10.1002/qj.2455

Maynard, T., 2015. Food System Shock: The Insurance Impacts of Acute Disruption to Global Food Supply. Lloyd's of London., London, UK.
Menon, A., Levermann, A., Schewe, J., Lehmann, J., Frieler, K., 2013. Consistent increase in Indian monsoon rainfall and its variability across CMIP-5 models. Earth Syst. Dyn. 4, 287–300. https://doi.org/10.5194/esd-4-287-2013
Ministerio de Agricultura, Ganaderia y Pesca de Argentina, 2015. Statistical database. URL http://www.siia.gov.ar/
Ministry of Agriculture and Farmers Welfare, Govt. of India, 2015. Crop Production Statistics. URL http://eands.dacnet.nic.in/
Mitchell, D., AchutaRao, K., Allen, M., Bethke, I., Forster, P., Fuglestvedt, J., Gillett, N., Haustein, K., Iverson, T., Massey, N., Schleussner, C.-F., Scinocca, J., Seland, Ø., Shiogama, H., Shuckburgh, E., Sparrow, S., Stone, D., Wallom, D., Wehner, M., Zaaboul, R., 2016a. Half a degree Additional warming, Projections, Prognosis and Impacts (HAPPI): Background and Experimental Design. Geosci. Model Dev. Discuss. 1–17. https://doi.org/10.5194/gmd-2016-203
Mitchell, D., James, R., Forster, P.M., Betts, R.A., Shiogama, H., Allen, M., 2016b. Realizing the impacts of a 1.5 [deg] C warmer world. Nat. Clim. Change.
National Bureau of Statistics of China, n.d. Regional data. URL http://data.stats.gov.cn/
Navarro-Racines, C.E., Tarapues-Montenegro, J.E., Ramírez-Villegas, J.A., 2016. BIAS-CORRECTION IN THE CCAFS-CLIMATE PORTAL: A DESCRIPTION OF MEHOTODOLOGIES.
Nelsen, R.B., 2007. An introduction to copulas. Springer Science & Business Media.
Nelson, G.C., Valin, H., Sands, R.D., Havlík, P., Ahammad, H., Deryng, D., Elliott, J., Fujimori, S., Hasegawa, T., Heyhoe, E., others, 2014. Climate change effects on agriculture: Economic responses to biophysical shocks. Proc. Natl. Acad. Sci. 111, 3274–3279.
Pathak, H., Wassmann, R., 2009. Quantitative evaluation of climatic variability and risks for wheat yield in India. Clim. Change 93, 157–175. https://doi.org/10.1007/s10584-008-9463-4
Podestá, G., Herrera, N., Veiga, H., Pujol, G., Skansi, M. de los M., Rovere, S., 2009. Towards a regional drought monitoring and warning system in southern South America: an assessment of various drought indices for monitoring the 2007-2009 drought in the Argentine Pampas.
Pope, V., Stratton, R., 2002. The processes governing horizontal resolution sensitivity in a climate model. Clim. Dyn. 19, 211–236. https://doi.org/10.1007/s00382-001-0222-8
Pope, V.D., Gallani, M.L., Rowntree, P.R., Stratton, R.A., 2000. The impact of new physical parameterizations in the Hadley Center coupled model without flux adjustments. Clim. Dyn. 17, 61–81.
Porter, J.R., Xie, L., Challinor, A.J., Cochrane, K., Howden, S.M., Iqbal, M.M., Lobell, D.B., Travasso, M.I., 2014. Food security and food production systems. In: Climate Change 2014: Impacts, Adaptation, and Vulnerability. Part A: Global and Sectoral Aspects. Contribution of Working Group II to the Fifth Assessment Report of the Intergovernmental Panel on Climate Change [Field, C.B., V.R. Barros, D.J. Dokken, K.J. Mach, M.D. Mastrandrea, T.E. Bilir, M. Chatterjee, K.L. Ebi, Y.O. Estrada, R.C. Genova, B. Girma, E.S. Kissel, A.N. Levy, S. MacCracken, P.R. Mastrandrea, and L.L.White (eds.)]. Cambridge University Press, Cambridge, United Kingdom and New York, NY, USA.
Power, S., Delage, F., Chung, C., Kociuba, G., Keay, K., 2013. Robust twenty-first-century projections of El Nino and related precipitation variability. Nature 502, 541–545. https://doi.org/10.1038/nature12580
Puma, M.J., Bose, S., Chon, S.Y., Cook, B.I., 2015. Assessing the evolving fragility of the global food system. Environ. Res. Lett. 10, 024007. https://doi.org/10.1088/1748-9326/10/2/024007
Ramteke, R., Gupta, G.K., Singh, D.V., 2015. Growth and Yield Responses of Soybean to Climate Change. Agric. Res. 4, 319–323. https://doi.org/10.1007/s40003-015-0167-5
Rogelj, J., Knutti, R., 2016. Geosciences after Paris. Nat. Geosci. 9, 187–189.

679 Rosenzweig, C., Elliott, J., Deryng, D., Ruane, A.C., Müller, C., Arneth, A., Boote, K.J., Folberth, C.,
680 Glotter, M., Khabarov, N., others, 2014. Assessing agricultural risks of climate change in the
681 21st century in a global gridded crop model intercomparison. Proc. Natl. Acad. Sci. 111,
682 3268–3273.
683 Rosenzweig, C., Ruane, A.C., Antle, J., Elliott, J., Ashfaq, M., Chatta, A.A., Ewert, F., Folberth, C.,
684 Hathie, I., Havlik, P., Hoogenboom, G., Lotze-Campen, H., MacCarthy, D.S., Mason-D'Croz, D.,
685 Contreras, E.M., Mller, C., Perez-Dominguez, I., Phillips, M., Porter, C., Raymundo, R.M.,
686 Sands, R.D., Schleussner, C.-F., Valdivia, R.O., Valin, H., Wiebe, K., 2018. Coordinating AgMIP
687 data and models across global and regional scales for 1.5C and 2.0C assessments. Philos.
688 Trans. R. Soc. Math. Phys. Eng. Sci.
689 Ruane, A.C., Antle, J., Elliott, J., Folberth, C., Hoogenboom, G., Croz, D.M.-D., Müller, C., Porter, C.,
690 Phillips, M.M., Raymundo, R.M., 2018. Biophysical and economic implications for agriculture
691 of+ 1.5 and+ 2.0 C global warming using AgMIP Coordinated Global and Regional
692 Assessments. Clim. Res. 76, 17–39.
693 Schaffnit-Chatterjee, C., Schneider, S., Peter, M., Mayer, T., 2010. Risk management in agriculture.
694 Dtsch. Bank Reseach Sept.
695 Schlenker, W., Roberts, M.J., 2009. Nonlinear temperature effects indicate severe damages to US
696 crop yields under climate change. Proc. Natl. Acad. Sci. 106, 15594–15598.
697 Schleussner, C.-F., Lissner, T.K., Fischer, E.M., Wohland, J., Perrette, M., Golly, A., Rogelj, J., Childers,
698 K., Schewe, J., Frieler, K., Mengel, M., Hare, W., Schaeffer, M., 2016a. Differential climate
699 impacts for policy-relevant limits to global warming: the case of 1.5 °C and 2
700 °C. Earth Syst. Dyn. 7, 327–351. https://doi.org/10.5194/esd-7-327-2016
701 Schleussner, C.-F., Rogelj, J., Schaeffer, M., Lissner, T., Licker, R., Fischer, E.M., Knutti, R., Levermann,
702 A., Frieler, K., Hare, W., 2016b. Science and policy characteristics of the Paris Agreement
703 temperature goal. Nat. Clim. Change 6, 827–835. https://doi.org/10.1038/nclimate3096
704 Schmitz, C., van Meijl, H., Kyle, P., Nelson, G.C., Fujimori, S., Gurgel, A., Havlik, P., Heyhoe, E., d'Croz,
705 D.M., Popp, A., Sands, R., Tabeau, A., van der Mensbrugghe, D., von Lampe, M., Wise, M.,
706 Blanc, E., Hasegawa, T., Kavallari, A., Valin, H., 2014. Land-use change trajectories up to
707 2050: insights from a global agro-economic model comparison. Agric. Econ. 45, 69–84.
708 https://doi.org/10.1111/agec.12090
709 Seneviratne, S.I., Donat, M.G., Pitman, A.J., Knutti, R., Wilby, R.L., 2016. Allowable CO2 emissions
710 based on regional and impact-related climate targets. Nature 529, 477–483.
711 https://doi.org/10.1038/nature16542
712 Sheffield, J., Goteti, G., Wood, E.F., 2006. Development of a 50-year high-resolution global dataset of
713 meteorological forcings for land surface modeling. J. Clim. 19, 3088–3111.
714 Sklar, M., 1959. Fonctions de répartition à n dimensions et leurs marges. Université Paris 8.
715 Tack, J., Barkley, A., Nalley, L.L., 2015. Effect of warming temperatures on US wheat yields. Proc.
716 Natl. Acad. Sci. 112, 6931–6936. https://doi.org/10.1073/pnas.1415181112
717 Tao, F., Yokozawa, M., Liu, J., Zhang, Z., 2008. Climate-crop yield relationships at provincial scales in
718 China and the impacts of recent climate trends. Clim. Res. 38, 83–94.
719 Ummenhofer, C.C., Xu, H., Twine, T.E., Girvetz, E.H., McCarthy, H.R., Chhetri, N., Nicholas, K.A., 2015.
720 How Climate Change Affects Extremes in Maize and Wheat Yield in Two Cropping Regions. J.
721 Clim. 28, 4653–4687. https://doi.org/10.1175/JCLI-D-13-00326.1
722 UNFCCC, 2015. Adoption of the Paris Agreement. FCCC/ CP/2015/10/Add.1. Paris, France. 1–32.
723 USDA, 2015. Economics, Statistics ad Market Information System.
724 Van Vuuren, D.P., Edmonds, J., Kainuma, M., Riahi, K., Thomson, A., Hibbard, K., Hurtt, G.C., Kram, T.,
725 Krey, V., Lamarque, J.-F., others, 2011. The representative concentration pathways: an
726 overview. Clim. Change 109, 5.
727 Verschuuren, J., 2016. The Paris agreement on climate change: Agriculture and food security. Eur J
728 Risk Reg 7, 54.
729 Von Braun, J., 2008. The food crisis isn't over. Nature 456, 701–701.

Zhang, T., Lin, X., Sassenrath, G.F., 2015. Current irrigation practices in the central United States reduce drought and extreme heat impacts for maize and soybean, but not for wheat. Sci. Total Environ. 508, 331–342.

Tables and Figures

Table 1. Pearson correlation coefficient between Princeton re-analysis climatological data and detrended, observed historical subnational crop yield data. ***, ** and * indicate $p < 0.01$, $p < 0.05$, and $p < 0.20$, respectively. Bold values indicate those properties that have been chosen as climate indicators in this paper.

	Wheat		**Maize**		**Soybean**	
	Maximum temperature	Precipitation	Maximum temperature	Precipitation	Maximum temperature	Precipitation
Argentina	**-0.493*** **	-0.140	**-0.602*** **	**0.645*** **	**-0.490*** **	**0.675*** **
Australia	**-0.356** **	**0.825*** **				
Brazil			-0.023	**0.260***	0.041	**0.392** **
China	0.237	**0.147**	**-0.157**	**0.335** **	-0.032	**0.137**
India	**-0.406*** **	**-0.195***	**-0.232***	**0.335** **	**-0.334** **	**0.533*** **
USA	-0.035	**0.309** **	**-0.293** **	**0.420*** **	**-0.208***	**0.330** **

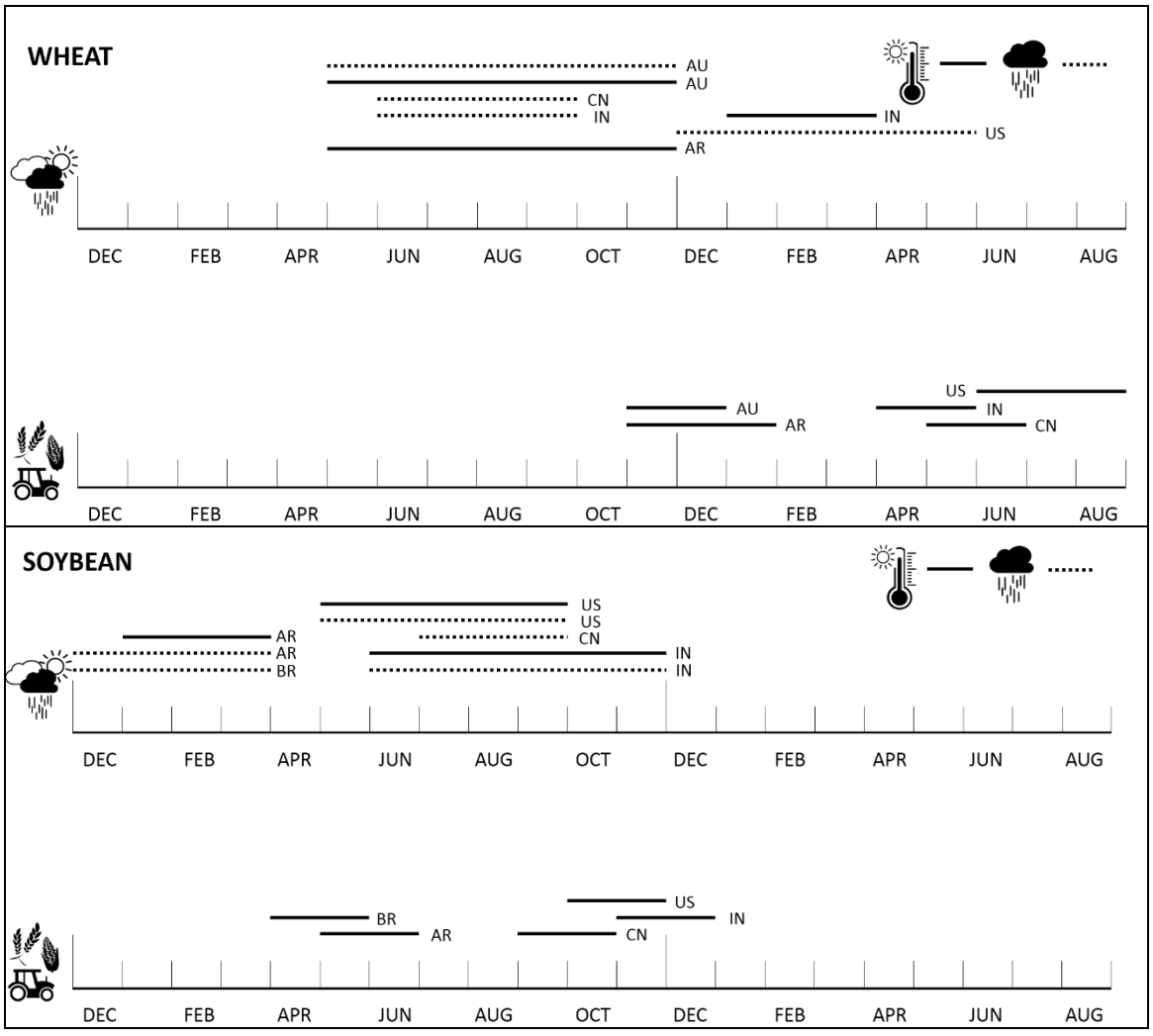

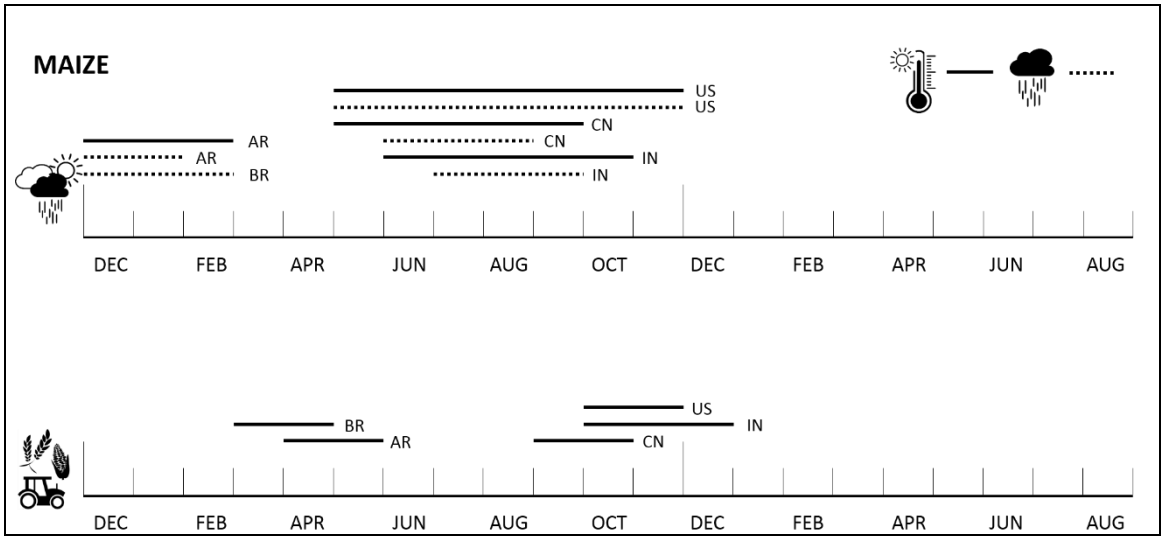

Figure 1. Climate indicators and harvesting periods for the global breadbaskets: Argentina (AR), Australia (AU), Brazil (BR), China (CN), India (IN) and the USA (US). Temperature-based indicators (continuous line) are monthly maximum temperature averaged over the crop growth relevant period. Precipitation-based indicators are cumulative precipitation over selected time periods (dashed line).

a)

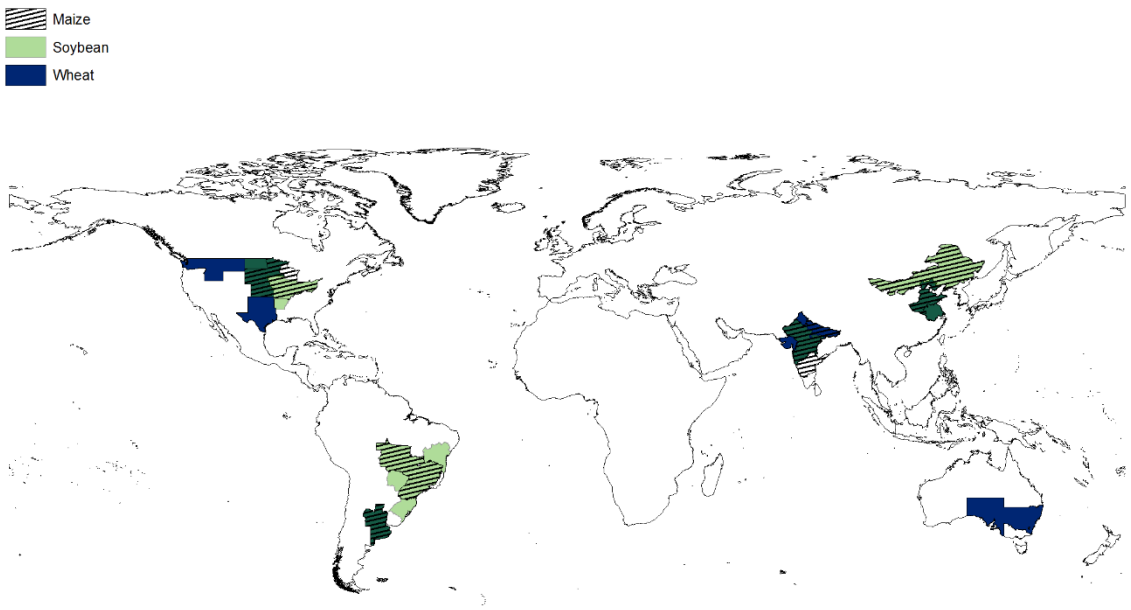
Maize
Soybean
Wheat

b)

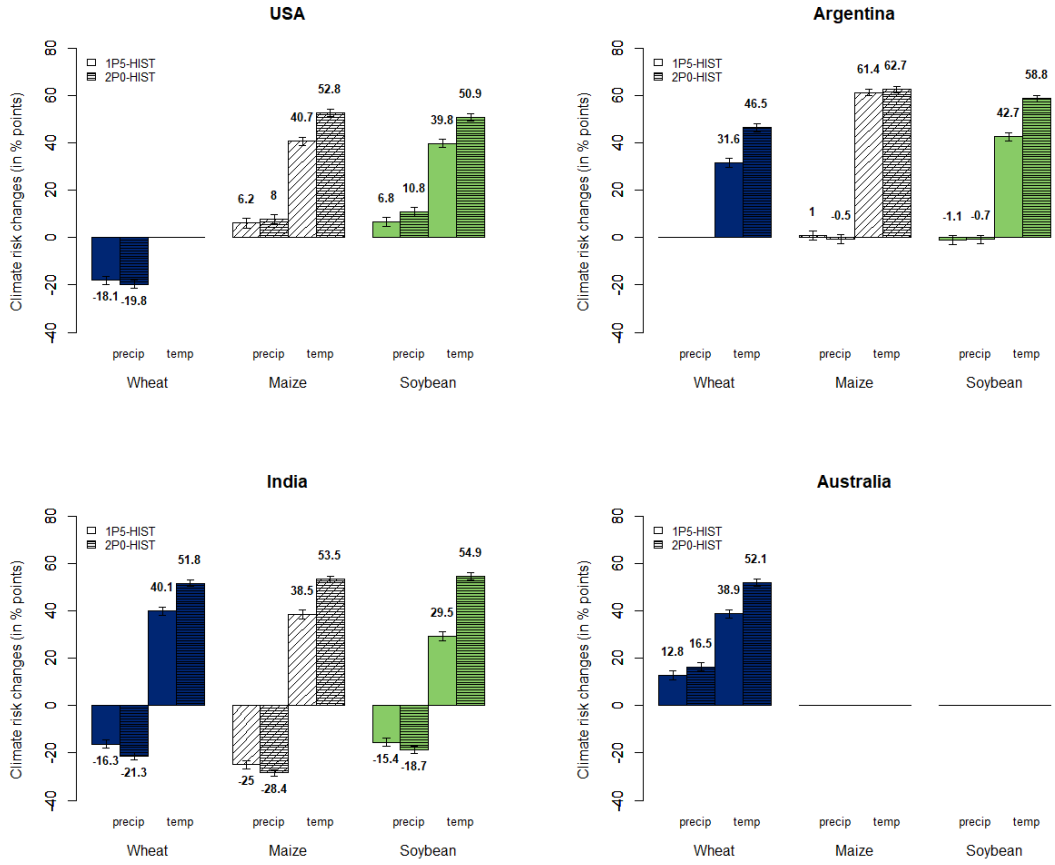
USA
Argentina
India
Australia
1P5-HIST
2P0-HIST
Climate risk changes (in % points)
precip
temp
Wheat
Maize
Soybean
-18.1
-19.8
6.2
8
40.7
52.8
6.8
10.8
39.8
50.9
31.6
46.5
1
-0.5
61.4
62.7
-1.1
-0.7
42.7
58.8
-16.3
-21.3
40.1
51.8
-25
-28.4
38.5
53.5
-15.4
-18.7
29.5
54.9
12.8
16.5
38.9
52.1

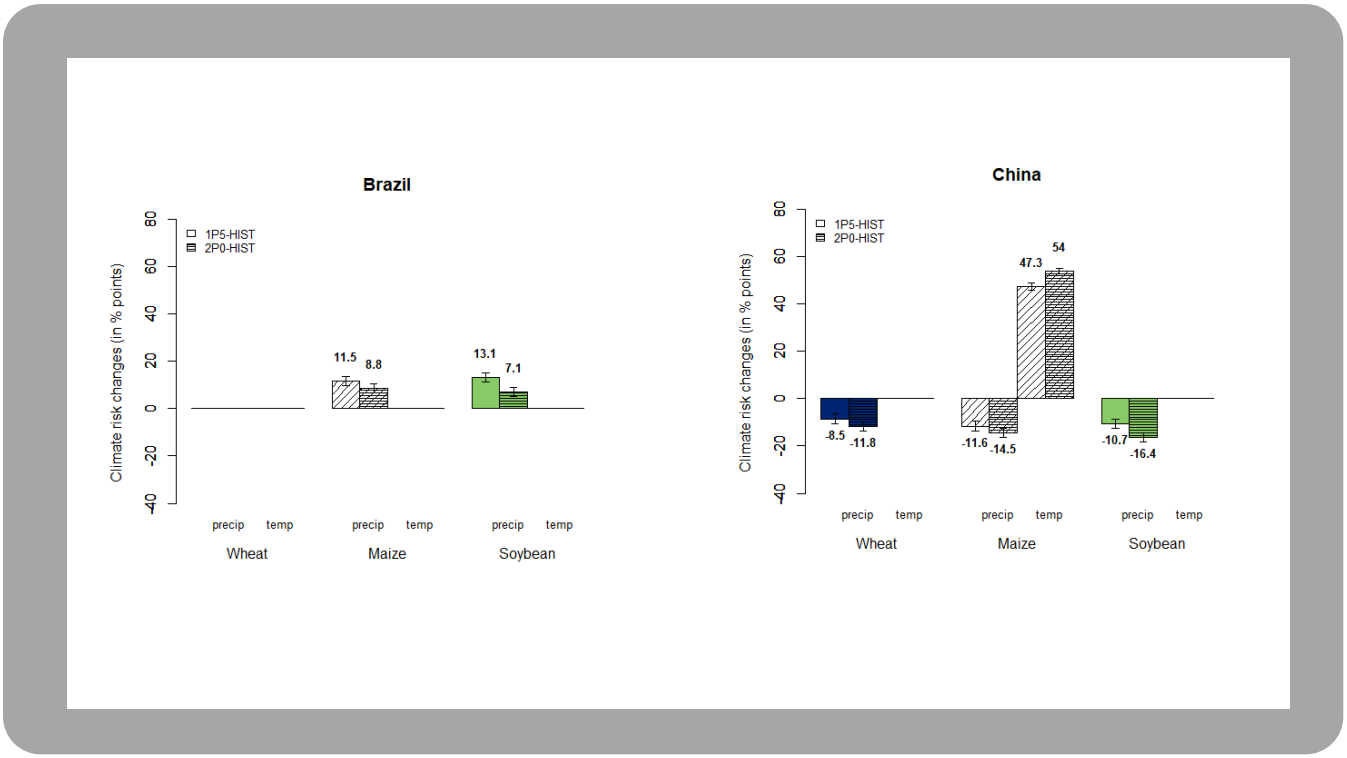

Figure 2. Changes in climate threshold exceedance between historical and 1.5 or 2 °C warming scenarios (in percentage points) using temperature and rainfall based indicators. A) shows the global breadbaskets for wheat, maize and soybean, b) summarizes the risk changes for the two warming scenarios. The error bar indicates the standard error between the 1000 iterations of threshold exceedance using resampled climate data. Using the KS test, all differences between the 1.5°C and 2°C scenarios are significant at a 0.001 significance level.

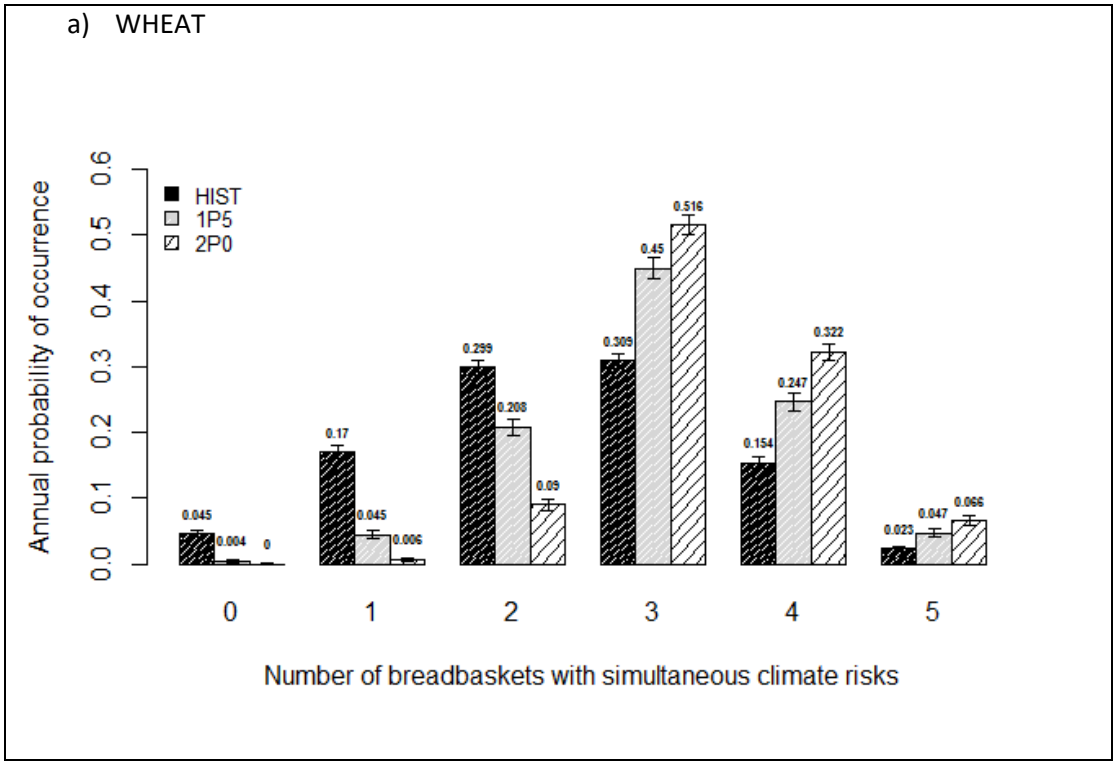

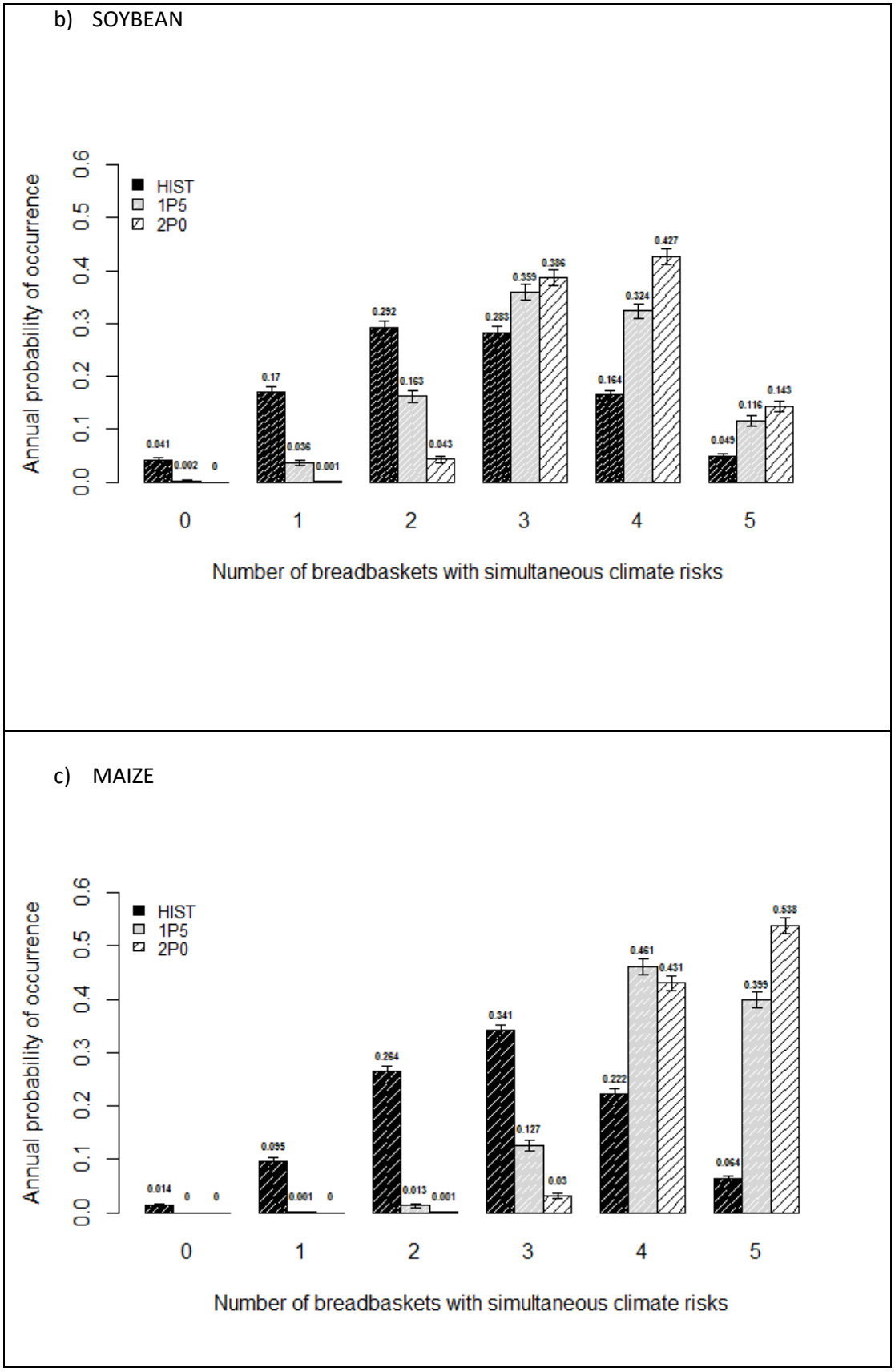

817

818 **Figure 3.** Risks of multiple breadbasket failure under 1.5 and 2°C warming. Error bars reflect the
819 sampling error as well as the copula simulation error which was determined in 1000 iterations.